Enabling A Hyper-Connected World: Advanced Antenna Design Using Liquid Crystals and LCD Manufacturing

Ryan A. Stevenson[1], Mohsen Sazegar[1], Phillip Sullivan[1]

ryan@kymetacorp.com
[1]Kymeta Corporation, 12277 134th Court NE, Redmond, WA, USA 98052
Keywords: 5G, Metamaterials, Liquid Crystal, Antennas.

ABSTRACT

5G is adopting low Earth orbit and geostationary satellite networks for global connectivity. Mobility applications require a highly directional, scanning user antenna to connect to these networks. We have commercialized a novel, scanning antenna technology, leveraging liquid crystal and LCD manufacturing to enable mass adoption and connectivity to these networks.

1 INTRODUCTION

The 5G network is intended to connect everyone and everything together, globally. However, terrestrial networks alone are unsuited to meet this goal due to restricted geographic coverage and capacity limitations [1]. Recent 5G working groups have adopted non-terrestrial networks (NTNs), and specifically non-geostationary orbit (NGSO) and geostationary orbit (GEO) satellite constellations as part of the 5G architecture [2]. NTNs must be utilized to realize the 5G goal of providing global, ubiquitous connectivity, and their role is expected to be explicitly defined in the upcoming 3GPP Release 17 standard.

While the 3GPP organization anticipates that satellite-based, non-terrestrial networks (NTNs) will augment 5G terrestrial networks for mobile platforms, the typical user equipment required to establish a satellite link to a moving automobile has, until now, made the idea completely impractical. Mobile satellite communications user equipment is dominated by parabolic antennas mounted on motorized gimbals. These solutions are too large, heavy, and power-consuming to offer solutions for consumer applications such as the connected automobile, or mobile user terminals for next-generation Low Earth Orbit (LEO) satellite constellations. The other alternative is phased array technology. This technology is unsuitable for consumer mobile applications however, due to high cost, power consumption, and the mass associated with thermal management solutions.

To address these limitations, we have commercialized an electronically scanned antenna technology, based on a diffractive metamaterials concept, called Metamaterial Surface Antenna Technology (MSAT). Electronic scanning is achieved using high-birefringence liquid crystals. The use of liquid crystals (LC) as a tunable dielectric at microwave frequencies permits large-angle (+/- 70° range) 2D beam scanning and fast tracking (~30°/sec), with antenna power consumption of < 35 Watts and antenna thickness ~ 5.0 cm and no moving parts. Kymeta's engineering approach, using LC and optimization of the materials and design for compatibility with liquid crystal display (LCD) manufacturing processes, positions the technology for mass production by leveraging the capital infrastructure of the LCD industry.

The remainder of this report is outlined as follows: Section 2 presents diffractive metasurfaces and holographic beam forming; Section 3 provides an overview of radio frequency liquid crystal (RFLC) materials and design considerations; Section 4 provides discussion of results and antenna performance; Section 5 concludes.

2 DIFFRACTIVE METAMATERIALS AND HOLOGRAPHIC BEAMFORMING

Recently, three-dimensional, refractive metamaterial approaches have been extended to two-dimensional surfaces, or metasurfaces [3]. Metasurfaces have several advantages over traditional bulk metamaterials, namely that they take up less physical space and have the potential for less-lossy structures. Metasurfaces are characterized by both the periodicity of scatterers and thickness of the surface being small relative to the wavelength of interest. We are leveraging the metasurface concept, in conjunction with diffractive beamforming principles to commercialize MSAT [4].

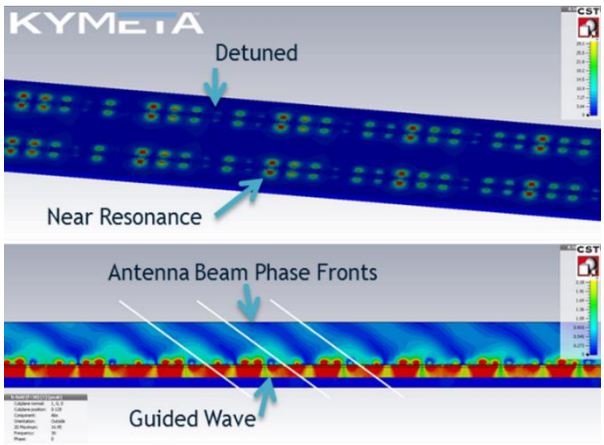

Fig. 1 Top view and cross section of the metasurface and feed waveguide

The MSAT approach is a metamaterials approach in which the antenna aperture is synthesized from a large number of sub-wavelength radiating elements. With MSAT (see Figure 1) each antenna element is coupled to a travelling wave feed structure comprised of a microwave waveguide. In the example shown in Figure 1, antenna elements are placed along the broad wall of a rectangular waveguide. Near their resonant frequency, the antenna elements couple energy from the feed wave and scatter this energy from the surface of the antenna. Antenna elements that have been detuned from their resonant frequency do not scatter energy from the feed wave. Due to the dense spacing of elements along the direction of the feed wave, elements with the correct phase to interfere constructively and produce radiation at the desired angle can be tuned to radiate (turned "on"). Elements with the undesired phase (otherwise resulting in destructive interference) can be detuned and prevented from radiating (turned "off"). The pattern of "on" and "off" elements, hence the antenna beam pointing angle and polarization state, can be changed dynamically in software.

The pattern of activated and deactivated antenna elements is determined from a holographic beam forming principle. In this formalism the feed wave is analogous to a reference beam (equation 1), and the wave coming off the antenna is analogous to an object beam (equation 2). Hence, the antenna surface becomes a diffractive grating, where the diffraction pattern is determined by the interference of these two waves (equation 3) [5]:

$$\Psi_{ref}(d) \approx exp\left(-i\vec{K}_s \cdot \vec{d}\right) \quad (1)$$

$$\Psi_{obj}(\vec{r}, \theta_o, \phi_o) = exp\left(-i\vec{K}_f(\theta_o, \phi_o) \cdot \vec{r}\right) \quad (2)$$

$$\Psi_{intf} = \Psi_{obj}\Psi^*_{ref} \quad (3)$$

In the equations above, $\vec{K}_s$ is the feed wave wavenumber, $\vec{K}_f$ is the free space wavenumber, which is a function of the desired azimuth and elevation scan angles and polarization, and * denotes the complex conjugate.

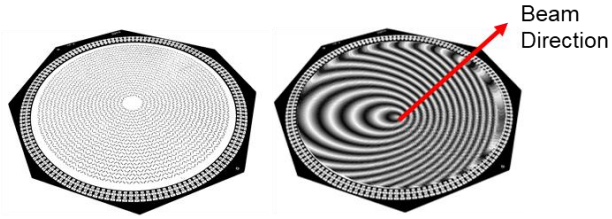

Fig 2. Calculated holographic diffraction pattern on a cylindrical metasurface

A graphic depiction of the holographic diffraction pattern calculated from equations 1-3 is shown in a cylindrical geometry in figure 2. The left figure depicts the metasurface and scattering elements. The right figure shows the calculated holographic diffraction pattern and associated scattering state for each antenna element in the metasurface array.

A key differentiator between MSAT and other resonant metamaterial phenomena is that the diffraction pattern on the metasurface is produced through tuning of element resonances, but the antenna beam is not produced on a resonance. Thus, the antenna bandwidth is not limited by the resonance of the elements themselves (a typical problem with resonant metamaterials) but by the tunability of the elements. MSAT, therefore, can achieve broadband operation as required for high-throughput satellite communications if the tuning mechanism can provide sufficient tuning range.

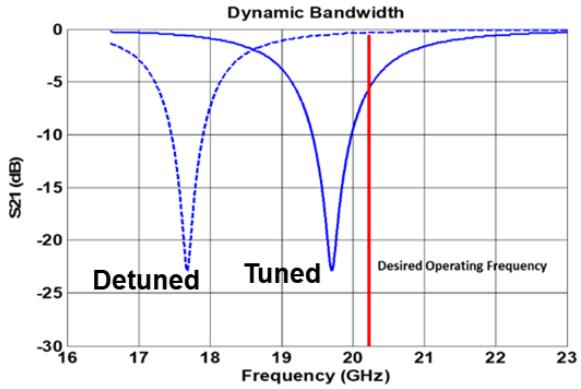

Fig. 3 Resonate state tuning between tune (strong scattering) and detuned (weak scattering) states

With each of the scattering antenna elements in the metasurface there is a portion of the capacitance of each element that is tunable, producing a resonant frequency shift as $1/\sqrt{L \cdot C}$, where L is the inductance of the antenna element and C is the capacitance. The capacitance of the antenna element is adjusted by using radio frequency liquid crystal (RFLC) as a tunable dielectric and varying the voltage across the antenna element.

Figure 3 is an insertion loss plot indicating the scattering strength of the antenna elements in either the tuned or detuned state at a desired operating frequency. For an antenna element near resonance (solid line), the high insertion loss indicates that energy is being radiated by the antenna element. For the detuned element (dashed line), the insertion loss is near zero, indicating that little energy is being radiated.

The amplitude contrast between tuned and detuned states at the operating frequency demonstrates how an amplitude hologram can be formed in the metasurface. The frequency separation and contrast between tuning states are directly related to the RFLC birefringence.

3 RADIO FREQUENCY LIQUID CRYSTALS

RFLCs typically consists of uniaxial nematic liquid crystals; however, for practical microwave device applications the bi-refringence is significantly larger than

conventional LC display liquid crystals. Prior work with LC-based microwave antennas has focused on producing phase shifters for phased-array antennas with improved figures of merit (FoM) over traditional microwave phase shifters [6]. The requirements for RFLCs in the MSAT approach are significantly different than with LC-based phase shifters. The FoM for LC phase shifters is heavily weighted towards reduced microwave losses, rather than large birefringence [7]. As discussed by Fritzsch, et. al., first generation microwave liquid crystals made incremental advances over traditional display liquid crystals (e.g., K15 and E7) in both tunability and loss, with two distinct development efforts to push for either lower loss or higher tunability [8]. MSAT requires large changes in the relative microwave permittivity with a tunability of roughly 35%-40%. The phase shifter approach, in contrast, sees tunabilities of typically ~20%, where the tunability is defined as:

$$\tau = \frac{\varepsilon_{||} - \varepsilon_{\perp}}{\varepsilon_{\perp}} \qquad (4)$$

In equation 4, $\varepsilon_{||}$ and $\varepsilon_{\perp}$ are the parallel and perpendicular microwave permittivity corresponding to the long axis and short axes of the LC molecule, as shown in Figure 4.

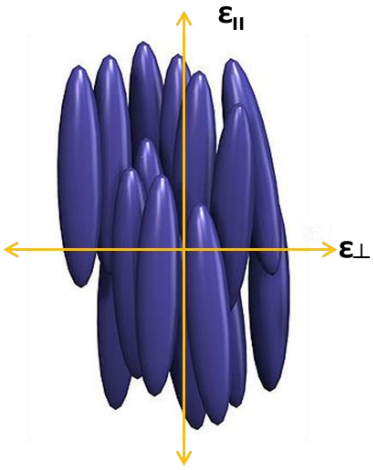

Fig. 4 RFLC geometric orientation and associated microwave permittivity

High birefringence LCs (hence large microwave tunabilities), are achieved through LC molecules with large electron polarizability anisotropy [9]. This effect is most prominent in molecules with long, conjugated π-electron systems. Molecules that optimize several important parameters tend to consist of rigid cores of benzene rings either directly connected or connected through an ethynyl bridge (tolane structure) as shown in Figure 5 [10].

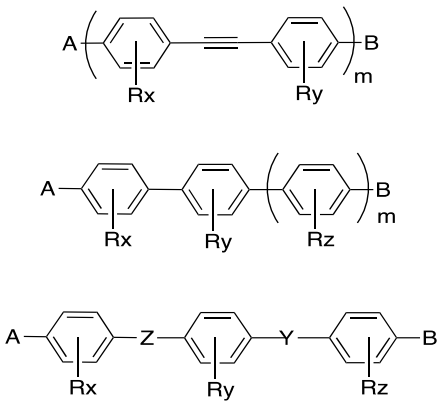

Fig. 5 General chemical core structures for high birefringence LCs

In Figure 5, the top and middle core structures are expressed in terms of units of number, m. All three structures can be laterally functionalized at the R positions, most commonly with protons, H, and/or heteroatoms such as fluorine, bromine, or chlorine. Alkyl groups, e.g. methyl, ethyl, or methoxy, ethoxy, etc. may be introduced at the various R positions as well. This lateral functionalization modifies intermolecular interactions to discourage smectic phase formation and/or to modify rotational viscosity, elastic constants, and melting point. Lengthening the core (increasing m) increases birefringence generally. Terminal functionalization has two primary considerations. First, to reduce the melting point and favor nematic phase formation, a long carbon tail is attached at the A position. Second, at the B position a polar end group, such as cyano (CN) or isothiocyanate (NCS) is used to further increase birefringence and introduce a permanent dipole.

4 MANUFACTURING AND ANTENNA PERFORMANCE

The metasurface construction, with an upper and lower substrate/electrode and LC as the tunable medium, closely resembles the assembly of an LC display. Array elements are individually addressed in an active matrix addressing scheme using printed thin film transistors (TFT), exactly as typical displays are made. The metasurface for our Ku-band product is currently produced on commercial LCD manufacturing lines. Figure 6 shows an antenna segment on a manufacturing line and the resultant antenna aperture assembly

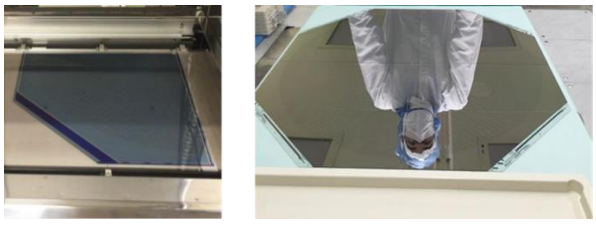

Fig. 6 An antenna segment in production and a complete antenna metasurface aperture

MSAT trades off discrete amplitude and phase control of each antenna element, as with phased array, for the manufacturability and cost of the diffractive metasurface approach. While dramatically lowering cost and power consumption over phased array and achieving consumer electronics scale manufacturing, MSAT has also demonstrated noteworthy technical capabilities for a flat-panel, electronically scanned antenna:

- Full duplex receive/transmit from a single physical aperture covering the extended Ku band
- Dynamic, software-adjustable from tracking linear to circular (RHCP and LHCP)
- Full 360° azimuth scanning and elevation scanning below 15° with return loss independent of scan angle
- Compliance with ITU and FCC power spectral density (PSD) masks

Figure 7 shows a broadside beam pattern for our Ku-band 80 cm antenna at 14.5 GHz, where compliance against the FCC mask is shown. Broadside receive performance achieves a dynamic bandwidth of 2.05 GHz (10.7-12.75 GHz), instantaneous bandwidth ~ 250 MHz, and peak G/T of 11.25 dB/K.

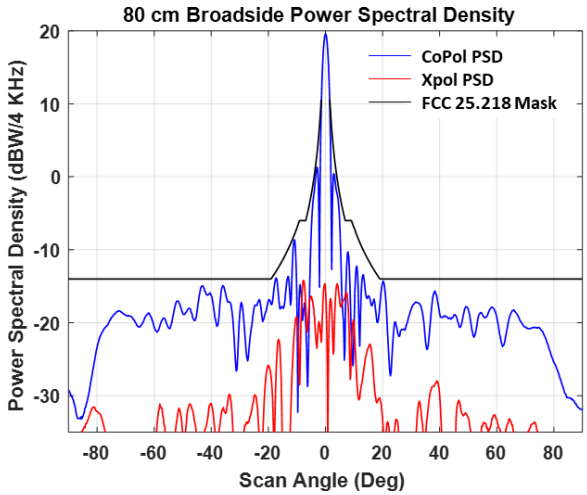

Fig. 7 Co-polarized and cross-polarized broadside power spectral density pattern normalized to 4 KHz bandwidth

5 CONCLUSION

With MSAT we have addressed the key technical challenges associated with 3D, resonant metamaterials and have demonstrated high-gain, electronically scanned arrays using RFLC and LCD manufacturing capabilities. The size, weight, power, performance, and manufacturing scale make MSAT well positioned to address high-volume, low-cost mobile satellite opportunities, which will make mobile NTN connectivity an integral part of the 5G architecture.

Fig. 8 Automobile integrated satellite terminal

REFERENCES

[1] Siegele, Ludwig, "The World in 2018," The Economist, pp. 126 (2018)

[2] "Study on New Radio (NR) to Support Non-Terrestrial Networks (Release 15)", 3GPP TR 38.811 v.0.2.1, November 2017

[3] C.L. Holloway, E.F. Keuster, J.A. Gordon, J. O'hara, J. Booth, and D.R. Smith, "An Overview of the Theory and Applications of Metasurfaces: The Two-Dimensional Equivalents of Metamaterials," IEEE Ant. Prop. Mag., Vol. 54, No. 2, pp. 10-35 (2012)

[4] K.M. Palmer, "Intellectual Ventures Invents Beam-Steering Metamaterials Antenna," IEEE Spectrum, November 30th (2011)

[5] M.C. Johnson, S.L. Brunton, N.B. Kundtz, J.N. Kutz, "Sidelobe Canceling for Reconfigurable Holographic Metamaterial Antenna," IEEE Trans. Ant. Prop., Vol. 63, No. 4, pp. 1881-1886, (2015)

[6] O. H. Karabey, et al., "Methods for Improving the Tuning Efficiency of Liquid Crystal Based Tunable Phase Shifters," Proc. 6th European Microwave Integrated Circuits Conference (EuMA 2011), pp. 494-497 (2011)

[7] S. Meuller, et al., "Broad-Band Microwave Characterization of Liquid Crystals Using a Temperature-Controlled Coaxial Transmission Line," IEEE Trans. Microwave Theory Tech, vol. 53, no. 6, pp. 1937-1945 (2005)

[8] Fritsch, C., Wittek, M., "Recent Developments in Liquid Crystals for Microwave Applications," 2017 IEEE Sym. Ant. Prop. (APS-2017), pp. 1217-1218 (2017)

[9] Dabrowski, R., Przemyslaw, K., and Herman, J., "High Birefringence Liquid Crystals," Crystals, Vol. 3, pp. 443-482 (2013)

[10] Sullivan, Philip A., et. al., "Antenna Having Radio Frequency Liquid Crystal (RFLC) Mixtures with High RF Tuning, Broad Thermal Operating Ranges, and Low Viscosity," US Patent No. 10,224,620